

Electrical and Structural Properties of Amorphous Germanium

J. J. Hauser and A. Staudinger

Bell Laboratories, Murray Hill, New Jersey 07974

(Received 2 January 1973)

The electrical conductivity of amorphous Ge films ranging in thickness between 240 Å and 6 μm was measured both in the plane and in the transverse directions. The Ge films were deposited by the getter-sputtering technique onto sapphire and glass substrates at the following temperatures: 573, 300, 170, and 77 °K. Transmission electron microscopy and x-ray diffraction were used to characterize the defect structure of films deposited by this technique and in this regard structural variations as a function of film thickness, substrate temperature, and substrate material were investigated. Most of the conductivity measurements were made on films deposited and kept at 77 °K; the annealing behavior of such films led to a better understanding of the defect structure and its influence on electrical properties. Marked differences were observed in electrical properties between films deposited at 300 °K and films deposited at 77 °K, which are related to the defect structure of the films. A marked anisotropy in both the resistivity and its temperature dependence was observed below 0.4 μm; this anisotropy increased with decreasing film thickness down to the thinnest film studied (240 Å).

I. INTRODUCTION

The purpose of this paper is to extend the previously published electrical-conductivity data¹ and present transmission electron micrographs and x-ray diffraction data in an effort to examine the possible relationship between the defect structure of sputtered amorphous Ge films and conductivity.

II. EXPERIMENTAL PROCEDURE

The experimental technique used in the deposition and in the electrical measurements of the films is the same as the one previously described.¹ The films were deposited on sapphire and glass substrates by the getter sputtering technique² from an arc-melted Ge target with a resistivity of 60 Ω cm. Although the starting vacuum was only in the low-10⁻⁷-Torr range, getter sputtering² results in much lower concentrations of such active gases as H₂O, O₂, and N₂. At any rate, these residual gases could not react with the films, as they are kept at 77 °K during deposition. The sputtering was performed at 2.25 W (1500 V, 1.5 mA) with an argon pressure of 1.5 × 10⁻² Torr. Thus, although the films are very pure from the point of view of H₂O, O₂, and N₂, they do contain somewhat less than 1 at.% of argon. Following deposition the film is transferred under liquid nitrogen onto the resistivity holder, which is then immersed in liquid helium. The resistivity of the film is then measured in helium gas at atmospheric pressure by warming up to room temperature. The temperature dependence of the resistivity is therefore obtained without exposing the films to air. For films deposited at 77 °K, the x-ray diffractometer trace was obtained by transferring the film under liquid nitrogen onto a cold copper finger partially immersed in a liquid-nitrogen bath contained in a

polystyrene box; in this way the x-ray diffraction data are obtained without warming the samples above 77 °K.

Transmission-electron-microscopy observations were all made at microscope ambient (~20 °C) and at an electron accelerating voltage of 200 kV. For these studies, films 25, 100, 300, and 600 Å thick were sputtered onto cleaved NaCl held at 300 °K, and, in addition, 100-Å films were sputtered onto NaCl substrates held at 77 and 473 °K. These films were floated free by dissolving the NaCl in distilled water and then they were mounted on 200-mesh rhodium-coated grids or "holey" carbon support films. In one instance a 1000-Å Pb film which had been evaporated onto a glass plate was used as a room-temperature substrate. In this case the Ge film was floated free by dissolving the Pb film in glacial acetic acid. This partition technique appears to be a very useful and general alternate technique to the most commonly used one involving alkali halide substrates, as acetic acid is a very mild etchant, which, as far as we know, dissolves very few metals besides lead. In still another experiment the Ge film was sputtered directly onto a supported holey carbon film, thereby avoiding the stripping operation.

III. EXPERIMENTAL RESULTS AND DISCUSSION

A. Structural Properties

Bright-field through-focus sequences were recorded from each of these films at an electron optical magnification of ≈ 100 000×. In a few instances micrographs suitable for stereoscopic examination were recorded. The results of these experiments indicate that for all films the observed defect-image contrast can be interpreted as arising from a three-dimensional network of pipelike channels

which have a lower mean potential than the surrounding matrix.³ This defect structure is therefore identified with density deficient regions (which from now on we shall call "cracks" for lack of a better name) and therefore from a contrast standpoint it is similar to that observed by Donovan and Heinemann⁴ in their structural study of evaporated amorphous germanium films.

All of the micrographs appearing in this paper were taken $\approx 3000 \text{ \AA}$ underfocused and in this imaging mode a crack appears "bright" relative to the average background level. Electron micrographs for 25-, 100-, 300-, and 600- \AA -thick films deposited at room temperature are shown in Fig. 1. In agreement with Donovan and Heinemann⁴ one sees dark areas which are surrounded by bright areas. These bright areas were identified by Donovan and Heinemann⁴ as being the crack network first suggested by Galeener.^{5,6} One important difference between the micrograph for the 100- \AA film shown in Fig. 1 and the one shown by Donovan and Heinemann⁴ for an evaporated 100- \AA film at 25 °C is that the dark areas are about 40 \AA in diameter in Fig. 1 versus 100 \AA in their case.⁴ The finer defect structure in the present films is believed to be caused by the sputtering process which in the case of crystalline films always leads to a finer grain size than evaporation. One also notices that the dark areas are smaller ($\approx 20 \text{ \AA}$) in the 25- \AA film [Fig. 1(a)] than in the 100- \AA film [Fig. 1(b)]; this would indicate that the defect structure becomes coarser with increasing film thickness. This coarsening seems to saturate around 100 \AA and lit-

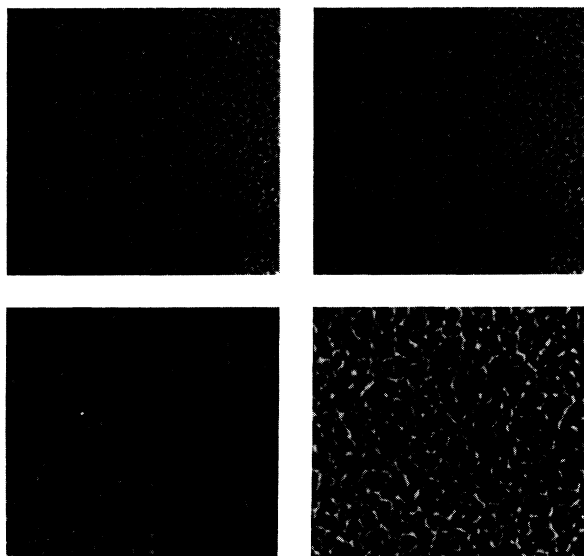


FIG. 1. Underfocused bright-field electron micrographs of Ge films deposited on NaCl substrates at 300 °K: (a) 25, (b) 100, (c) 300, and (d) 600 \AA thick.

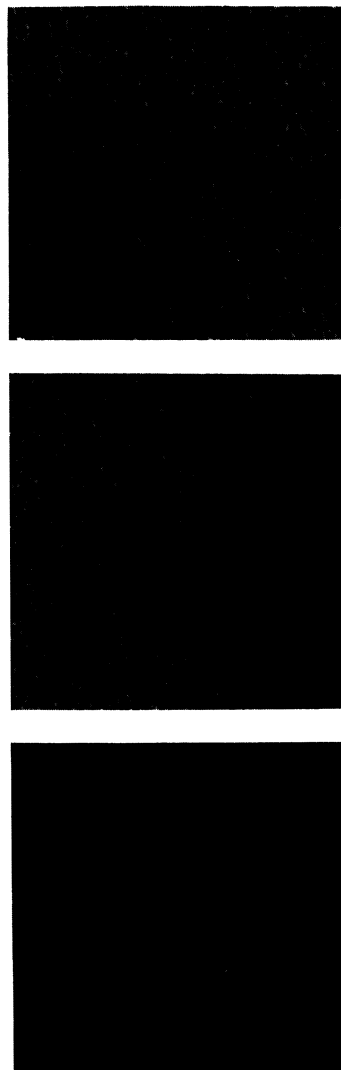


FIG. 2. Underfocused bright-field electron micrographs of 100- \AA -thick Ge films deposited on NaCl substrates at (a) 77, (b) 300, and (c) 473 °K.

tle coarsening seems to develop thereafter, as one can judge by comparing the electron micrograph of Fig. 1(b) for the 100- \AA film with those of Figs. 1(c) and 1(d) pertaining to the 300- and 600- \AA films; of course, the dark areas in the 600- \AA films could be appreciably thicker than those of the 100- \AA film. The influence of the temperature of deposition is studied in Fig. 2. A film deposited at 77 °K and warmed up to room temperature [Fig. 2(a)] looks very much the same as a film deposited at 20 °C [Fig. 2(b)]. Consequently, even if cracks are absent in a film deposited at 77 °K, as will be suggested later, they are certainly present after annealing to room temperature. The electron micrograph shown in Fig. 2(c) for a film deposited at 200 °C disagrees with Donovan and Heinemann⁴ in



FIG. 3. Underfocused bright-field electron micrographs of 100-Å-thick Ge films deposited onto (a) NaCl, (b) Pb, and (c) amorphous carbon all held at 300°K.

two ways. First, they reported⁴ that the dark areas get larger with increasing deposition temperature, which is certainly not the case in Fig. 2(c); second, they found that the cracks disappear when a film is evaporated at 200°C, while the cracks are clearly seen in Fig. 2(c). These differences can again be ascribed to the different deposition processes, sputtering versus evaporation: it is a well-known fact that the atomic mobility is much lower in a sputtered film than in an evaporated film, principally because of the presence of argon during sputtering.

A point which has been raised many times is whether the cracks revealed by the electron micrographs are due to the fact that the Ge films are always grown on an alkali halide substrate. In order to partially answer this question we have used a

new partition technique using a Pb-film substrate. It can be seen from Fig. 3(b) that the cracks are still present for the film grown on Pb and, more generally, that the defect structure and its scale are quite similar for the films grown on NaCl [Fig. 3(a)] and on Pb [Fig. 3(b)]. One may further question the existence of these cracks in a Ge film still lying on its substrate. This question is partially answered by the experiment where a 100-Å Ge film was deposited on a holey carbon film; the resulting structure [see Fig. 3(c)] is identical to that shown in Fig. 3(a), thereby proving that the cracks do not occur as a result of floating the film from the substrate and that the cracks are present in thin films regardless of the type of substrate (alkali halide, Pb, or C).

It has already been pointed out that from the standpoint of conductivity¹ a film deposited at 77°K is quite different from one deposited at room temperature and that the former changes appreciably upon annealing. It is therefore important to characterize the structure of a film deposited at 77°K without warming it up. The x-ray diffraction data taken at 77°K on a film deposited at 77°K is compared in Fig. 4 with the diffraction pattern also taken at 77°K on a film deposited at 300°K. There was essentially no difference between the x-ray patterns taken at room temperature or at 77°K on the film deposited at 300°K; as there is no temperature dependence of the x-ray diffraction, Fig. 4 only shows patterns taken at 77°K to simplify the comparison. The x-ray diffraction for the room-temperature-deposited film leads to conclusions similar to the ones reached by electron diffractions on evaporated films.⁴ There are two diffraction peaks: one very close to the crystalline Ge (111) line and

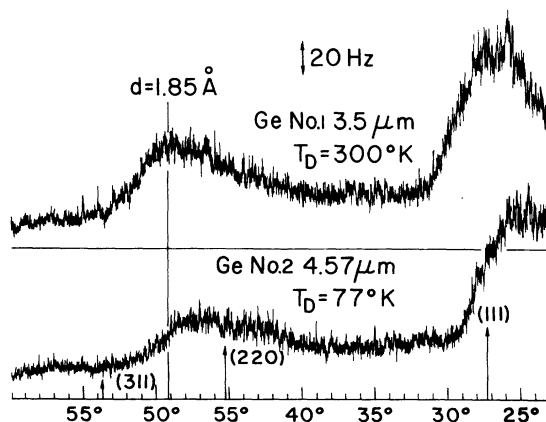


FIG. 4. X-ray diffractometer traces taken at 77°K for two Ge films, one deposited at 77 and the other at 300°K. The trace for the film deposited at 77°K was obtained at 77°K without warming up the film; the arrows indicate the positions of the diffraction peaks for crystalline Ge.

another one at $d \cong 1.85 \text{ \AA}$ compared with Ge (220), $d = 2.00 \text{ \AA}$ and Ge (311), $g = 1.70 \text{ \AA}$. While these peaks remain essentially unchanged for films grown between 25 and 250 °C, it is clear from Fig. 4 that the film deposited at 77 °K has a considerably more distorted structure: the intensity of the peaks over background is about half and the peaks are more diffuse and further displaced towards smaller angles (lower density). Therefore Fig. 4 establishes that the atoms coming down at 77 °K are quite frozen in, as one would expect from the fact that diffusion is quite unlikely at that temperature. Galeener suggested⁵ as the origin for cracks that during growth of the film, two islands of ideally amorphous material are unable to coalesce because atoms cannot satisfy the angle and distance necessary for an ideal tetrahedral bond. One would assume that such a process would at least require adatom diffusion which may not be present at 77 °K. In view of the very distorted nature of the x-ray pattern shown in Fig. 4 for the film deposited at 77 °K, one may expect that atoms between two islands would rather make improper bonds (wrong angle and/or wrong interatomic distance) rather than create a crack. If such a film is annealed at room temperature, this energetically unfavorable situation results in cracks as shown in Fig. 2(a). It is of course possible that diffusionless microcracks are present even in a film deposited at 77 °K, but one would expect such cracks to be much narrower than those found on films deposited or annealed at room temperature. The difference between a planar region filled with pairs of bad bonds and a crack of zero width is only of academic interest and it seems safe to speculate that films deposited at 77 °K do not have the defect structure on the scale shown in Figs. 1–3.

B. Electrical Properties

The temperature dependence of the planar resistance for films deposited and kept at 77 °K is shown in Fig. 5. These data overlap with those presented in Ref. 1 (see Fig. 2) and extend the data to films as thin as 50 Å. As shown in Fig. 5, the data for films deposited at 77 °K are very well fitted below 120 °K by the relation

$$\rho = \rho_0 e^{(T_0/T)^{1/4}}, \quad (1)$$

where T_0 [given by $16\alpha^3/N(E_F)k$] is approximately equal to 10^8 K , appreciably lower than the value of T_0 ($3 \times 10^8 \text{ K}$) for room-temperature-deposited films; α is the coefficient of exponential decay of localized states, $N(E_F)$ is the density of localized states at the Fermi level, and k is Boltzmann's constant. The parameters pertinent to the planar resistance of films deposited at 77 and 300 °K are summarized in the first portion of Table I both for

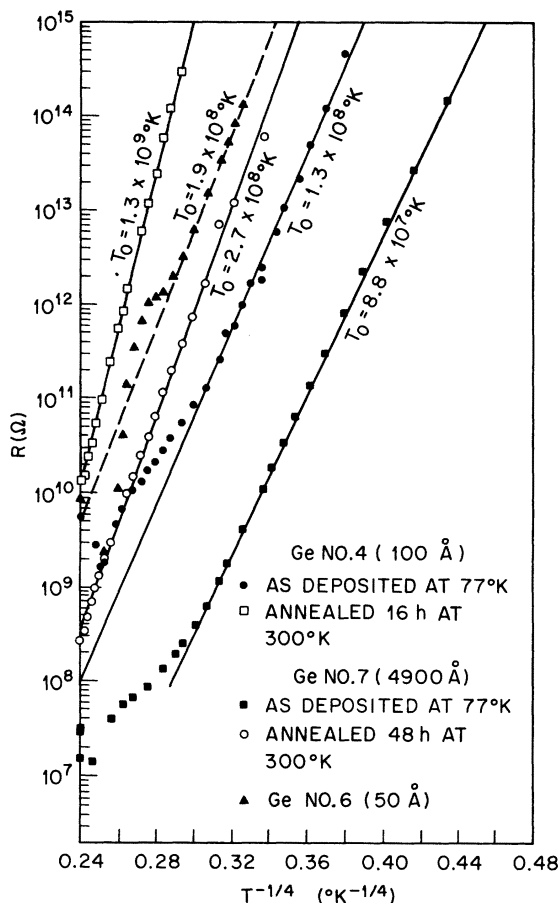


FIG. 5. Temperature dependence of the planar resistance for films deposited at 77 °K showing the effect of room-temperature annealing. For Ge samples 7, 4, and 6, $\rho_{\text{extr RT}} = 35, 80,$ and $2000 \text{ } \Omega \text{ cm}$, respectively.

the films studied in Ref. 1 and for the present work. The films anneal around 120 °K as shown by the deviation from the low-temperature data towards higher resistance. If one extrapolates the low-temperature data to room temperature for films thicker than 100 Å, one obtains a $\rho_{\text{extr RT}}$ on the order of a few tens of $\Omega \text{ cm}$, which is lower than the value for room-temperature-deposited films (see Table I). After annealing at room temperature the films regain values of the appropriate parameters which are characteristic of a room-temperature-deposited film (see Table I, where the values of ρ_0 and T_0 for evaporated films^{7,8} are given for comparison at the bottom of the table). Taking into account the defect structure characterized by electron and x-ray diffractions, one can obtain a consistent rationalization of the electrical properties and the annealing effects. One may postulate that films deposited at 77 °K possibly have low-density regions of the type described by Car-gill,⁹ but no cracks. The x-ray diffraction (Fig.

TABLE I. Properties of Ge films.

Film and sample No.	d_{Ge} (Å)	T_D^a (°K)	ρ_{RT}^b (Ω cm)	T_0 (°K)	ρ_0 (Ω cm)
Ge _{0.99} Ga _{0.01} 1	58 000	300	600	2.9×10^8	1.4×10^{-11}
Ge 1	35 000	300	1500	3.2×10^8	1.7×10^{-11}
Ge 8	300	300	6000	5.5×10^8	6.3×10^{-13}
Ge 9	28 600	573	600	2.7×10^8	2.5×10^{-11}
Ge 2	45 700	77	57	9.3×10^7	3.2×10^{-9}
Ge 2			11 100	2×10^8	4.3×10^{-9}
annealed ^c 48 h					
Ge 7	4900	77	35	8.8×10^7	2.7×10^{-9}
Ge 7					
annealed 48 h			11 600	2.7×10^8	4.9×10^{-10}
Ge 3	300	77	14.4	10^8	5.2×10^{-10}
Ge 3					
annealed 16 h			9360	2.6×10^8	5.2×10^{-10}
Ge 4	100	77	80	1.3×10^8	5.8×10^{-10}
Ge 4					
annealed 16 h			11 200	1.3×10^9	1.7×10^{-16}
Ge 6	50	77	2 000	1.9×10^8	1.1×10^{-9}
Cd-Ge-Cd 1	3720	77	1.9	6×10^7	1.2×10^{-8}
Cd-Ge-Cd 1					
annealed to 300 °K			66	9.7×10^7	2.9×10^{-9}
Cd-Ge-Cd 1					
annealed 48 h			280	10^8	10^{-8}
Pb-Ge-Pb 6	3570	77	1.3	5.8×10^7	10^{-9}
Pb-Ge-Pb 6					
annealed to 193 °K			8	9×10^7	5.5×10^{-10}
Pb-Ge-Pb 7	1770	77	1.2	5.1×10^7	1.8×10^{-9}
Pb-Ge-Pb 8	900	77	2.2	4.1×10^7	9.8×10^{-9}
Pb-Ge-Pb 8					
annealed to 153 °K			6	6×10^7	3.9×10^{-9}
Pb-Ge-Pb 9	420	77	4.3	3.3×10^7	5.3×10^{-8}
Pb-Ge-Pb 9					
annealed to 300 °K			98	1.1×10^8	2×10^{-9}
Pb-Ge-Pb 10	240	77	1.35	2.5×10^7	5.5×10^{-8}
Mg-Ge-Mg 1	450	77	6.4	3.6×10^7	5.3×10^{-8}
Mg-Ge-Mg 2	340	77	10	1.1×10^7	9.8×10^{-6}
Mg-Ge-Mg 3	240	77	10	1.25×10^7	6.2×10^{-6}
Ag-Ge-Mg 1	240	77	3.75	3.2×10^7	5.3×10^{-8}
Pb-Ge-Pb 5	5850	300	550	2.4×10^8	5.6×10^{-11}
Pb-Ge-Pb 1	5000	170	11	1.8×10^8	9×10^{-12}
Pb-Ge-Pb 2	2950	170	18	1.7×10^8	2.2×10^{-11}
Pb-Ge-Pb 4	1500	170	36	1.5×10^8	10^{-10}
Pb-Ge-Pb 3	1250	170	29	1.5×10^8	1.3×10^{-10}
Chopra and Bahl ^d				10^8	5.7×10^{-9}
Walley and Jonscher ^e				7.2×10^7	10^{-8}

^aTemperature of deposition of the film.

^bRoom-temperature resistivity for a film deposited or annealed at 300 °K, $\rho_{extr RT}$ for films deposited at 77 °K (see text).

^cAnneal was performed at 300 °K unless otherwise indicated.

^dReference 7.

^eReference 8.

4) at 77 °K suggests a more distorted structure where atoms would be frozen in during deposition, thus leading to a greater density of localized states (thus lower T_0), but where adatom mobilities⁵ would be too low for crack formation. Upon annealing two phenomena occur simultaneously: localized states are annealed out, thus increasing T_0 , and crack formation occurs [Fig. 2(a)]. At

this point, one can already suggest that the cracks do not have a major influence on the electrical conduction in films thicker than 100 Å. Indeed, the increase in resistivity taking place upon annealing can be mostly explained by the increase in T_0 , leaving ρ_0 approximately constant. The same argument will be made later on about the annealing experiments in the transverse direction. Actually,

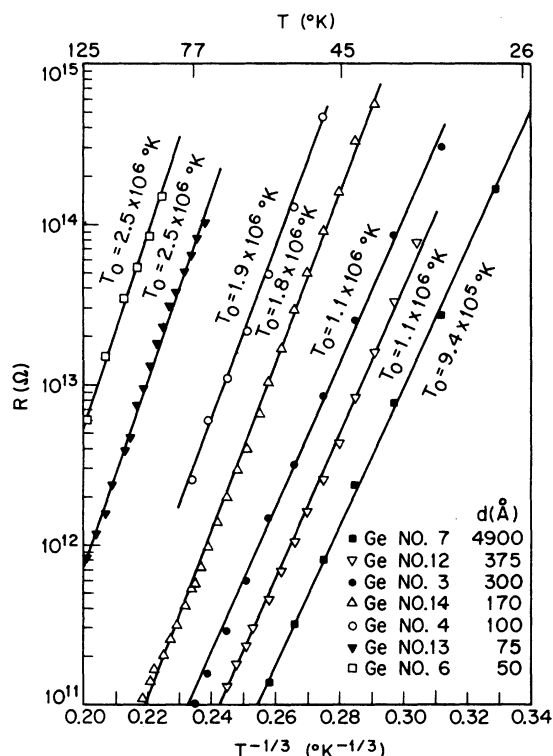


FIG. 6. Temperature dependence of the planar resistance for very thin films ($d \leq 375$ Å) deposited at 77 °K compared with the temperature dependence of a thick Ge film (4900 Å).

as one can see from Table I, ρ_0 is not always constant but is just as likely to increase or decrease upon annealing. As there is, however, no reliable theory linking the prefactor ρ_0 to any defect structure of the films, it seems safe to conclude that the cracks contribute at most an isotropic term to the prefactor. This point seems further confirmed by the fact that the resistivity after annealing is constant for films ranging in thickness between 4.6 μm and 100 Å (Table I); if cracks on the scale of 40 Å [Fig. 1(b)] affected the electrical conduction, one would expect the resistivity of the 100-Å film to be appreciably higher than that of thicker films. This point will be further discussed in conjunction with the transverse resistance measurements.

It is already apparent from Table I that T_0 starts to increase with diminishing film thickness for films thinner than 300 Å deposited at 77 °K. This point is further established in Fig. 6, where more films have been studied in the appropriate thickness range; the effect seems to start at $d \approx 300$ Å and for films thinner than 300 Å, T_0 is approximately proportional to the inverse square root of the thickness. This effect can be explained in two possible ways. The first explanation is based on the fact that the defect structure of such thin films changes

with film thickness. Indeed, as shown in Fig. 1, appreciable coarsening takes place in the first 100 Å. Of course, this behavior may only be typical of films deposited at room temperature [or annealed at room temperature as shown in Fig. 2(a)] and may not be characteristic of the films described in Fig. 6, which were deposited and kept at 77 °K. Nevertheless, if such coarsening takes place in films deposited at 77 °K, it could then explain the increase in T_0 . Relating a higher T_0 with a finer defect structure is based on the previous empirical observation that room-temperature-sputtered films which display a finer defect structure than room-temperature-evaporated films [compare Fig. 1(b) with Fig. 1 of Ref. 4] also have a three times larger T_0 value (see Table I). On the other hand, Shante¹⁰ has recently considered the planar electrical conduction in very thin films. His argument is based on the fact that the electron hopping distance increases with decreasing temperature and that at low temperatures the conduction in very thin films will change from a three- to a two-dimensional behavior essentially because the hopping distance becomes comparable with the film thickness. In the two-dimensional regime, Shante predicts that the exponent $\frac{1}{4}$ in relation (1) changes to $\frac{1}{3}$ and that T_0 is inversely proportional to the film thickness. A similar increase in resistivity was found in amorphous carbon films¹¹ thinner than 500 Å and was attributed to a transition to two-dimensional flow. The change in exponent from $\frac{1}{4}$ to $\frac{1}{3}$ in the two-dimensional case has been derived by Hamilton.¹² It is apparent from Fig. 6 that the data are well fitted by relation (1) with the exponent $\frac{1}{4}$ replaced by $\frac{1}{3}$. This is, however, no proof for the validity of Shante's theory, as a 4900-Å-thick film which is too thick for his theory to apply is fitted just as well with exponent $\frac{1}{4}$ (Fig. 5) or $\frac{1}{3}$ (Fig. 6). This last point simply emphasizes that one cannot really distinguish between these two exponents in this temperature range; consequently Fig. 6 only establishes that the data could be fitted with exponent $\frac{1}{3}$ in agreement with theoretical predictions. On the other hand, it is obvious from Fig. 6 that in agreement with theoretical predictions¹⁰ T_0 increases with decreasing thickness (d); the experimental functional dependence ($T_0 \propto d^{-1/2}$) is different from theoretical predictions ($T_0 \propto d^{-1}$). This last discrepancy could, however, result from the interplay between some structural change occurring in such thin films and the two-dimensional behavior.

The temperature dependence of the transverse resistance for films deposited and kept at 77 °K is shown in Fig. 7. The data are very similar to the data shown in Fig. 3 of Ref. 1, which were obtained with Pb electrodes. The parameters which refer to the transverse resistance of films deposited at

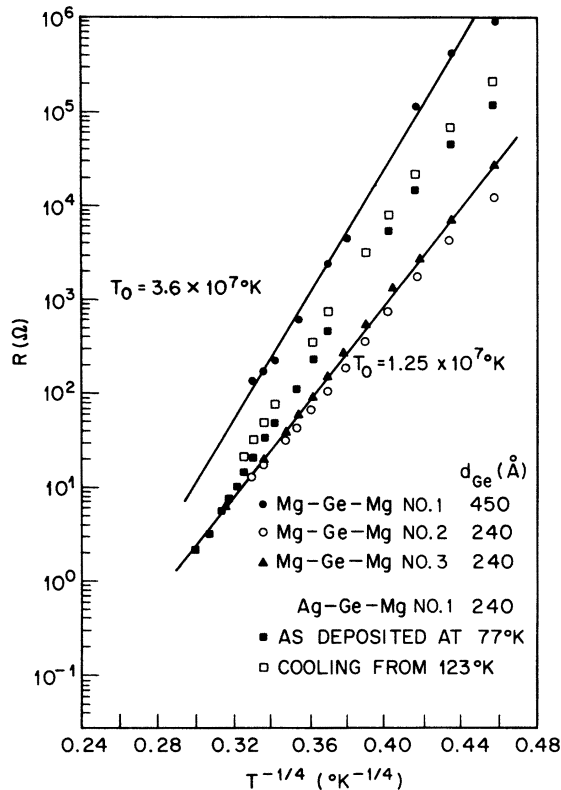


FIG. 7. Temperature dependence of the transverse resistance for films deposited at 77°K showing the effect of room-temperature annealing. For the three Mg sandwich samples 1, 2, and 3 and the Ag-Mg sandwich, the $\rho_{\text{extr RT}}$ are 6.4, 10, 10, and 3.75 Ω cm, respectively.

77°K are summarized in the second portion of Table I both for the films studied in Ref. 1 and for the present films. If one compares these data with the planar measurements, one observes a marked anisotropy, which reveals itself in two ways for films thinner than 4000 Å. First of all, T_0 decreases smoothly from 6 to 1.1×10^7 °K, as the film thickness decreases from 4000 to 240 Å, respectively. These values of T_0 should be compared to $T_0 = 10^8$ °K for the planar measurements. These results are independent of the electrode material as Pb, Cd, Mg, and Ag give similar results. Furthermore, $\rho_{\text{extr RT}}$ is now a few Ω cm versus a few tens of Ω cm for the planar measurements.

One could think that the anisotropy, i. e., the difference in resistivity and in T_0 , arises from the different preparations used in the planar and transverse geometries. Indeed, while the planar measurements are made on films deposited on glass or sapphire, the transverse measurements are obtained on a Ge film comprised between two electrodes. The direct effect of electrodes can be ruled out by the facts that the transverse measure-

ments are independent of electrode material and that the transverse measurements on films thicker than 4000 Å are similar to the planar measurements. The indirect effect of electrodes such as protection of the Ge film from gas contamination can be ruled out as well for the following two reasons. First, the anisotropy has been established¹ on films made and kept under liquid nitrogen and measured up to 120°K without any sign of annealing. Consequently the presence of ambient inert helium gas should have no effect whether the film is protected by an electrode or not. Second, the electrical properties of amorphous Ge are especially affected by air exposure but such exposure was avoided in both planar and transverse measurements. The exposure to argon during the sputtering of the films as we saw previously results in a slight increase in T_0 as compared to vacuum-evaporated films. The anisotropy in the transverse measurements which results in a progressive decrease of T_0 in a thickness range (4000–300 Å) where the T_0 for planar measurements is essentially constant could therefore hardly be ascribed to the presence or absence of helium gas. The data obtained for Ag-Ge-Mg 1 by heating up to 123°K (Fig. 7) is almost reversible upon cooling, which demonstrates again that the curves are reversible if the annealing temperature (123°K) is not exceeded. As can be seen from Table I, the increase in resistivity upon annealing to room temperature can be mostly accounted for by an increase in T_0 , and although ρ_0 is not exactly constant, it is again as likely to increase or decrease upon annealing. Once more this suggests that the cracks present in annealed thin films do not appreciably affect the electrical-conduction mechanism. In the case of Cd-Ge-Cd 1 the room-temperature anneal increased T_0 to 10^8 °K and ρ to 280 Ω cm (Table I); this is still somewhat below the corresponding planar measurements. The anisotropy disappears around 5000 Å, as revealed by transverse measurements on Pb-Ge-Pb 5 deposited at room temperature (see Fig. 8 and Table I), yielding parameters ($T_0 = 2.4 \times 10^8$ °K and $\rho_{\text{RT}} = 550$ Ω cm) identical to those in the planar measurements. The anisotropy in the conductivity of thinner films is consistent with inhomogeneities on a semimacroscopic scale in the plane of the film, extending up to several thousand angstroms perpendicular to the plane. It was previously suggested that cracks are most probably not present in films deposited at 77°K; this assumption seems confirmed by the anisotropy which begins at a thickness of 4000 Å, much larger than the observed scale of the cracks. On the other hand, this anisotropy would be consistent with the 2000-Å-long cylindrical low-density regions suggested by Cargill.⁹

The temperature dependence of the transverse

resistance as a function of temperature for films deposited at 170 °K and one film deposited at 300 °K is shown in Fig. 8. It is clear that the properties of the films deposited at 170 °K are intermediate between those of films deposited at 300 and 77 °K. Focusing on Pb-Ge-Pb 1, we see that $T_0 = 1.8 \times 10^8$ °K is intermediate between 3×10^8 °K for room-temperature-deposited films and 6×10^7 °K for films deposited at 77 °K; on the other hand, $\rho_{\text{extrRT}} = 11 \Omega \text{ cm}$ is also intermediate between 550 and 2 $\Omega \text{ cm}$. Furthermore, one sees again a small anisotropy in T_0 for films thinner than 5000 Å, although there is no clear trend on ρ_{extrRT} . These experiments are convincing evidence that the structural changes occurring in the low-temperature-deposited films increase monotonically as the deposition temperature is lowered from 300 to 77 °K. Annealing Pb-Ge-Pb 3 to 200 °K and cooling down reveals again the increase in resistivity and in T_0 resulting from the annealing of localized states.

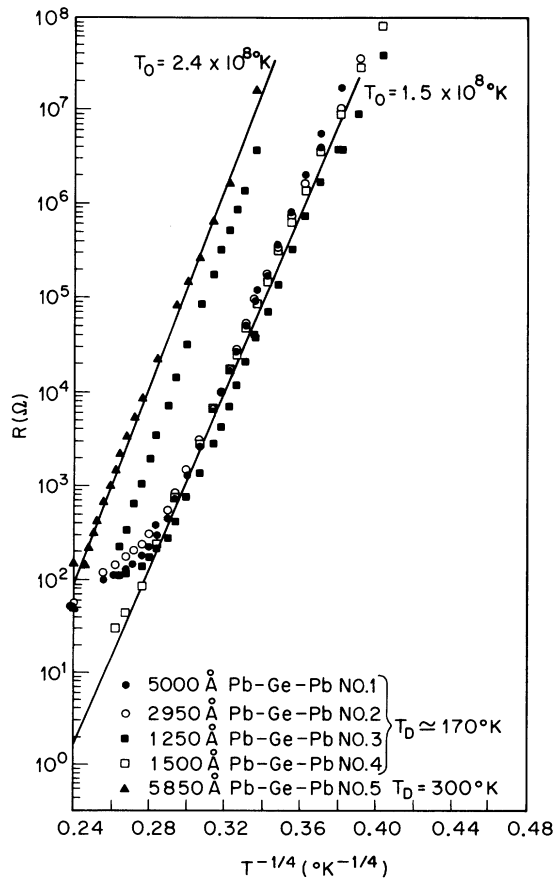


FIG. 8. Temperature dependence of the transverse resistance for films deposited at 170 and 300 °K. The ρ_{extrRT} for the four samples 1, 2, 3, and 4 deposited at 170 °K are 11, 18, 29, and 36 $\Omega \text{ cm}$, respectively. The ρ_{RT} for sample 5 deposited at 300 °K is 550 $\Omega \text{ cm}$.

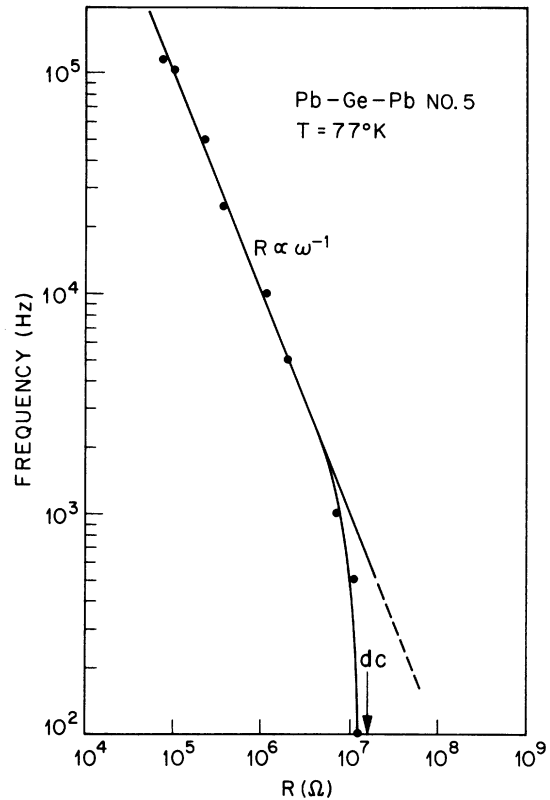


FIG. 9. Frequency dependence of the resistance for a sample deposited at 300 °K.

Finally, the frequency dependence measured at 77 °K on Pb-Ge-Pb 5 deposited at 300 °K is shown in Fig. 9. The data show that the ac resistivity decreases with frequency ω as ω^{-1} above a frequency of 2000 Hz. This is consistent with a hopping conductivity proceeding via single hops. These data are also in excellent agreement with those reported by Chopra and Bahl⁷ on evaporated films.

In summary, we found that Ge films deposited or annealed at 300 °K and of thickness up to 600 Å have a defect structure consisting of a three-dimensional network of density deficient channels (pipes, cracks, etc.) which coarsens with increasing film thickness. It seems that these cracks have little if any influence on the electrical conduction except possibly in ultrathin films. All Ge films regardless of deposition temperature have a temperature-dependent resistivity which is well fitted by relation (1). Films deposited at 77 °K have a lower value for T_0 as a result of greater disorder; it also seems likely that such films are crack-free. A marked anisotropy in both the resistivity and its temperature dependence was observed below a film thickness of 0.4 μm , which would tend to link this anisotropy to the type of

defect structure proposed by Cargill.⁹ The understanding of electrical conduction in amorphous semiconductors will be hopefully improved by performing a similar study on Si and Si-Ge alloys. These experiments will be the subject of a future publication.

ACKNOWLEDGMENTS

We are indebted to D. Maher for many useful discussions on the electron microscopy and for his contribution to the manuscript. We would also like to thank J. H. Wellendorf and J. E. Bernardini for their technical assistance.

¹J. J. Hauser, Phys. Rev. Lett. **29**, 476 (1972).

²H. C. Theuerer and J. J. Hauser, J. Appl. Phys. **35**, 554 (1964).

³D. M. Maher and A. Staudinger (unpublished).

⁴T. M. Donovan and K. Heinemann, Phys. Rev. Lett. **27**, 1794 (1971).

⁵F. L. Galeener, Phys. Rev. Lett. **27**, 1716 (1971).

⁶F. L. Galeener, Phys. Rev. Lett. **27**, 421 (1971).

⁷K. L. Chopra and S. K. Bahl, Phys. Rev. B **1**, 2545 (1970).

⁸P. A. Walley and A. K. Jonscher, Thin Solid Films **1**, 367 (1968).

⁹G. S. Cargill, III, Phys. Rev. Lett. **28**, 1372 (1972).

¹⁰V. K. S. Shante, Phys. Lett. **43A**, 249 (1973).

¹¹C. J. Adkins and E. M. Hamilton, in *Proceedings of the Second International Conference on Conduction in Low-Mobility Materials, Eilat, Israel, 1971* (Taylor and Francis, London, 1972), p. 229.

¹²E. M. Hamilton, Philos. Mag. **26**, 1043 (1972).

Electron-Paramagnetic-Resonance Studies on Arsenic Acceptors in Natural (2H) and Synthetic (3R) MoS₂ Crystals

R. S. Title and M. W. Shafer

IBM Thomas J. Watson Research Center, Yorktown Heights, New York 10598

(Received 12 March 1973)

We have observed the EPR spectra of As acceptors in both natural MoS₂ crystals (2H polytype) and in synthetic MoS₂ crystals (3R polytype). The *g* values of the resonance signals show that the As acceptors are associated with a band that has *d*_{z²} orbital character. Energy considerations indicate that the As acceptors are most likely substitutional on sulfur sites. The observation of *d*_{z²} orbital character for the As acceptors on sulfur sites is only consistent with a MoS₂ band structures that has the *d*_{z²} band as the highest filled band. In one of our samples the concentration of As acceptors was low enough so that some of the holes introduced by the As acceptors were localized at the As impurity. For these centers we were able to observe an As⁷⁵ hyperfine structure in the EPR spectrum. We determine from this hyperfine structure a value of $\langle 1/r^3 \rangle = 2.99$ a.u. for the hole orbit around the As and a value for the nuclear electric quadrupole moment of As⁷⁵, *q* = 0.28 b.

INTRODUCTION

The wide range of electrical properties ranging from insulating through semiconducting to superconducting that are found in the structurally and chemically similar layered transition-metal dichalcogenides has attracted considerable experimental and theoretical interest.¹ There have been several proposals of band-structure models which attempt to explain the electrical, optical, and other properties of these materials. While none of these has been completely successful in explaining all the properties, the proposed band-structure schemes have been very useful in providing a framework for discussion and for establishing some physical understanding of the properties.

The band structures that have been proposed are made up of molecular orbitals composed from the orbital wave functions on the transition-metal and the chalcogen atoms. Some of the proposed models are shown in Fig. 1. In these models the valence band *V* is made up primarily of the chalcogen *s* and *p* orbitals; the conduction band *C* is made up pri-

marily of the transition-metal *s* and *p* orbitals; and the nonbonding and antibonding transition-metal *d* orbitals are either in the forbidden gap or else overlap the conduction or valence bands. The ordering of the *d* orbitals is determined by the crystal symmetry at the metal site. The order shown in Fig. 1 is appropriate for the trigonal prismatic structure found for group-V and group-VI dichalcogenides such as NbS₂ and MoS₂. The number of

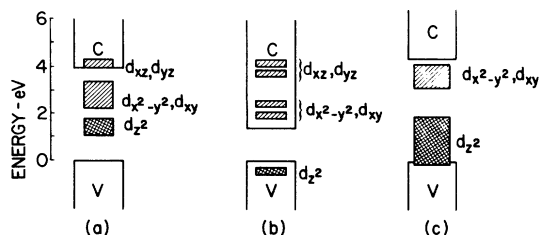


FIG. 1. Proposed band-structure schemes for MoS₂ (a) following Wislon and Yoffe (Ref. 1); (b) following Huisman *et al.* (Ref. 2); (c) following McMenamin and Spioer (Ref. 3).

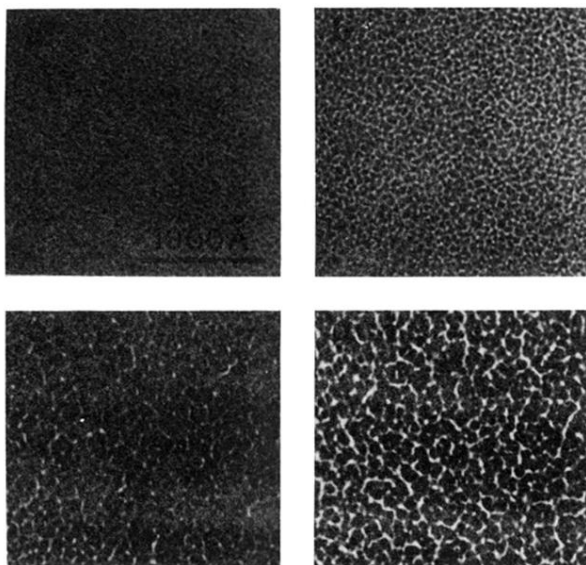


FIG. 1. Underfocused bright-field electron micrographs of Ge films deposited on NaCl substrates at 300 °K: (a) 25, (b) 100, (c) 300, and (d) 600 Å thick.

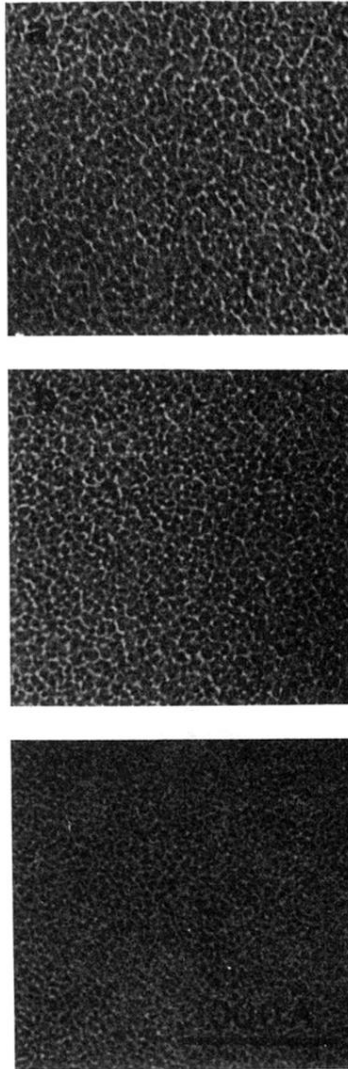


FIG. 2. Underfocused bright-field electron micrographs of 100-Å-thick Ge films deposited on NaCl substrates at (a) 77, (b) 300, and (c) 473 °K.

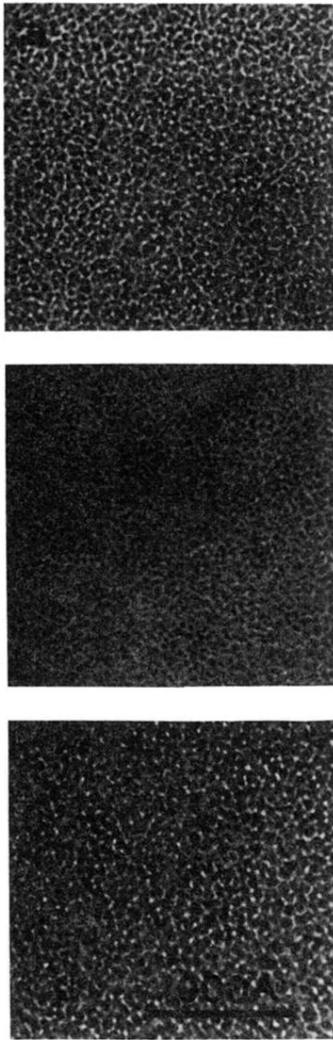


FIG. 3. Underfocused bright-field electron micrographs of 100-Å-thick Ge films deposited onto (a) NaCl, (b) Pb, and (c) amorphous carbon all held at 300°K.